72nd International Astronautical Congress (IAC), Dubai, United Arab Emirates, 25-29 October 2021.


IAC-21,C2,2,12,x63981

# On-Orbit Manufacturing of Large Space Structures Using Solid Foams

**Peter G.B. Hastie [a]*, Gilles Bailet [a], Colin R. McInnes [a]**

[a] Space and Exploration Technology Group, James Watt School of Engineering, *University of Glasgow, Glasgow G1228QQ, United Kingdom*
** Corresponding Author 2591092H@student.gla.ac.uk*

**Abstract**
The development of on-orbit manufacturing processes will enable the fabrication of large space structures that are free from many of the constraints of deployable structures, for example overcoming the volume limitation of the launch vehicle payload faring. Such structures could be designed to better suit applications such as photovoltaic (PV) power generation, antennae or solar reflectors by providing large rigid planar surfaces. These surfaces could be on a scale significantly larger than might otherwise be possible with deployables. However, to optimise such planar structures the mass of their support structures must be minimised, while providing adequate mechanical properties. This paper will consider the use of solid foams to provide an interesting material for the support of large planar structures. The dispersed nature of foams means that they can be stored in a small volume, but provide a large volume on formation for a low mass. This characteristic has seen the adoption of foams for terrestrial high strength, low weight applications. Additionally, the rapid production of foam allows for short fabrication times when compared to other on-orbit manufacturing processes, such as additive layer manufacturing. Following a discussion of the opportunities presented by foams, this paper will consider case studies where the foam is used as both a thermal and a structural component. These case studies explore the manufacturing parameters of these processes to understand the system requirements of the different methods considered. In each study solid foams were found to have lower construction times and energy requirements than other method of in-orbit manufacturing. This suggests the use of solid foams in missions that require short commissioning times and low power generation capabilities.

**Nomenclature**
$\rho$ = Density
$\varphi$ = Foam to solid relative density
$\sigma$ = Tensile stress
$\tau$ = Shear stress
F = Force
M = Moment
p = Pressure
E = Elastic modulus
G = Bulk modulus
$\nu$ = Possion's ratio
$I_n$= Second moment of area around neutral axis n
$R_T$ = Thermal resistance
T = Temperature
Q = Heat flux

**Acronyms/Abbreviations**
Mechanical Ground Support Equipment (MGSE), Additive Manufacturing (AM), Physical Vapour Deposition (PVD), Polyurethan (PU), Fused Disposition Method (FDM), Direct Energy Deposition (DED), Ultra-Violate (UV), Finite Element (FE), Computed Tomography (CT), PolyVinyl Chloride (PVC), International Space Station (ISS)

## 1 Introduction

In-space manufacturing methods have been of growing interest over the past few decades [1]. One of the critical applications of in-space manufacturing is in the construction of macro-scale structures in-space. The translation of manufacturing processes from the surface of the Earth into orbit enables the construction of such macro-scale structures by removing the limitations imposed on the structure by both the launch and ground environments. Structures that are manufactured in-space do not have to be packed into deployable configurations inside a launch vehicle payload faring and then survive the significant loads experienced during launch. Hence in-space manufactured structures could achieve much higher packing ratios when compared to deployable structures, since only bulk materials may need to be launched. In addition, structures manufactured in micro-gravity do not have to be designed to support themselves against their own weight as would be the case on the ground. As such, macro-scale structures manufactured in-space do not have the same strength requirements that similarly sized structures would require on the ground. While many deployable space structures already take advantage of the free-fall environment in-orbit, often MGSEs are required for deployment test and storage on the ground. As a result, structures that are manufactured in orbit would not need to consider either ground or launch loads.

To take full advantage of the large length-scale and low mass structures that in-space manufacturing offers, work has been carried out into ways to reduce the mass of material used and increase the packing

ratio – the scale of the final volume delivered when compared to the initial payload volume. This has included the development of AM process that would be suitable for the in-orbit environment [2] [3], and could be used to produce mass optimised 3D printed structures as well as exploring PVD of thin films [4]. This paper will explore solid foams as a material that could be used in the construction of large structures in orbit and which in principle offers a number of key advantages.

The paper will discuss the properties of solid foams (section 2), potential applications for solid foams in-orbit (section 3), how foams compare to other materials proposed for these applications via the discussion of case studies (section 4) and the next steps and future opportunities for solid foams in orbit (section 5).

## 2 Solid Foams

Solid foams are solid materials with gas filled voids (cells) in a 3D pattern throughout the material [5]. The mixture of solid structure and gas cells mean that solid foams have a lower density than their respective bulk solid materials. The relative density ($\varphi=\rho_{Foam}/\rho_{Solid}$) of a solid foam when compared to its bulk solid material is fundamental to both the material properties of the foam [5] and the foam's packing ratio. Another way to describe the relative density of the foam is its inverse – the expansion ratio. Foams with a low relative density and high expansion ratio can occupy much greater volume than the same mass of solid material. This is illustrated in Figure 1, each of the 3 cubes have the same mass of raw material, however their enveloped volume varies inversely with their relative density. When considering the manufacturing of solid foams, this reduction in mass also means a reduction in feed stock, energy and the time required to produce a given volume of material. Some solid foams have a relative density that is less than 0.1 [6], hence expansion ratios of greater than 10 may be achievable. This increase in volume means an increase in all dimensions of the structure and so could also imply an increase in thickness, length, cross-sectional area and second moment of area, all of which could be advantageous in a range of applications.

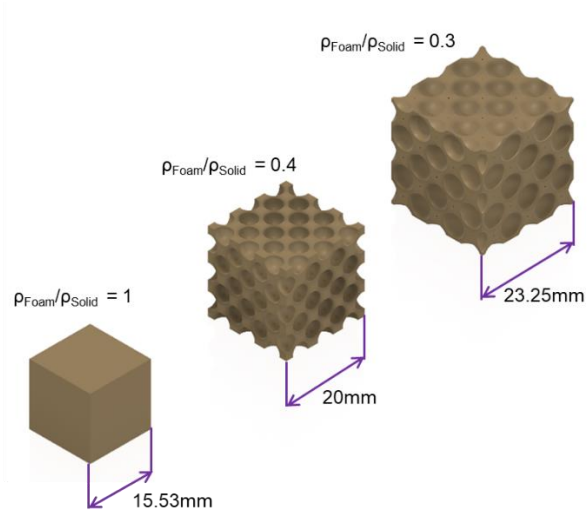


*Figure 1 – Foam expansion ratio example*

There are associated changes with the material properties of solid foams due to their relative density [5]. The nature of the 3D pattern of cells and structure of the solid material is also important to the bulk material properties of the solid foam [7].

### *2.1 Solid Foam Manufacturing*

There are several manufacturing methods that will produce solid foams. The process used to create a solid foam is highly dependent on the solid material that will be produced. Synthetic foams can be broken into three categories based on the material produced: ceramic foams, metal foams and polymeric foams.

Ceramic [8] and metal foam [9] manufacturing processes often require casting of material. Given the high energy demands of casting, this paper will focus on polymeric foams. Polymeric foams can further be divided into two groups [10]: thermoplastic foams and thermo setting foams.

The manufacturing processes for each of these polymeric foams differs in how the respective polymer solidifies. For a thermal plastic foam, the liquid-gas foam is rapidly cooled so that the plastic material hardens around the gas cells before the gas can defuse. In the case of a thermal setting foam, the liquid-gas foam consists of a mixture of resins which cure into a solid polymeric foam. Both manufacturing processes produce the solid foam via an initial liquid foam stage. In both cases the liquid foam is created by injecting the liquid with a gas known as a blowing agent.

There are many methods for introducing the blowing agent into the liquid foam. The blowing agent can be introduced into the liquid gas in a pressurised or supercritical state, such as is described for PEEK foam manufacturing by Cafiero et al [11] or for polycarbonate foam manufacturing by Ma et al [12]. In some cases the blowing agent is generated via

chemical reactions. In the case of polyurethane foams, this chemical reaction occurs in the presence of a catalyst [13]. Chemical reaction blowing agents can also be activated via UV exposure [14] [15] or heating [16].

As discussed, two of the advantages of solid foams for in-space manufacturing are that they could allow for a high packing ratio and that foams could require less energy to form material than alternative manufacturing processes. Thermoset polymeric foams with reaction released blowing agents appear to take best advantage of solid foam manufacturing with high packing ratios and low volumetric energy costs. Some of these processes do not require high power consumption as the energy required for both blowing agent generation and curing is provided via chemical reactions. In some cases, these reactions require activation via UV radiation, which is of particular interest given the intensity of UV radiation in the space environment. Thermoset polymeric foams also provide excellent packing ratios as the pre-processed resin can be transported as a liquid with a much higher density than the foam they produce [6]. Thermal setting foams also have rapid production times with some foams forming dimensionally stable shapes after 80-120s [17]. The foam developed by Schlögl et al [15] is of particular interest as both the blowing agent generation and polymer curing was activated using UV. The foaming process in this example was carried out at room temperature.

### *2.2 Solid Foam Structures*

The structure of the solid material in a solid foam is highly dependent on the process and material used. In most cases solid foams are formed from an initial liquid foam that is then solidified before the blowing agent can dissipate. As such the final solid foam structure is a result of the development of a liquid foam and the solidification process.

The structure of a liquid foam is a result of the equilibrium between the gas cell gauge pressure and the surface tension at the liquid-gas boundary [18]. As surface tension is proportional to area, the structure of the liquid foam is determined by the minimisation of surface area for a given liquid fraction. As the liquid fraction decreases the most energy efficient structure moves from a ’wet foam‘, when the cells are spherical and packed as incompressible spheres, to a ‘dry foam’ when the cells are no longer spherical and are separated by thin films of liquid that follow Plateau's laws [19]. As well as the liquid fraction, the liquid foam structure is also affected by the range of cell sizes in the foam. Given the closely packed nature of liquid foams, large variations in cell size will affect the arrangement of the liquid foam structure. Foams with a small range of cells sizes are referred to as monodisperse and foams with a large range of cell sizes are polydisperse. While in a liquid stage the foam structure can develop and change under the influence of drainage, gas dissipation, cell ripening and cell coalescence [20].

During solidification, the rapid material property changes in the solid material can lead to rupturing of the thin-film boundaries between cells [21]. The number of cells in a foam for which the cell wall ruptures is dependent on the development of the shear modulus in the solid material, the pressure of blowing agent and the thickness of the cell walls (which is related to the foam relative density or liquid fraction). If more than half the cells in a foam are open then the foam is considered to have an open foam structure, whereas a foam where more than half of its cells have intact cell walls is described as a closed cell foam. Whether a solid foam has a closed or an open cell structure is significant in the bulk properties of the foam [5]. Open cell foams are typically more flexible than close cell foams made of the same material, for example flexible polyurethan has an open cell structure [21], [22]. The relative size of the cells in the foam also has an impact on the properties of the solid foam [23].

### *2.3 Mechanical Properties*

As discussed, the material properties of the foam are dependent on the relative density and microstructure of the foam as well as the solid material used. A great deal of research has been carried out to understand the effect of these properties on the mechanical properties of bulk solid foam. This has been carried out via both empirical studies [24], [25] and theoretical modelling [26], [27]. A popular theoretical model for estimating the mechanical properties of solid foams was proposed by Gibson and Ashby [5] and is referred to as the Gibson-Ashby model. The model represents the solid foam as a series of cubic cells. The model then considers the mechanical properties of this cubic model as a function of the relative density of the foam. In the case of an open foam, all the remaining solid mass of the foam is modelled as being part of the cell channels, which in the cubic model is the edges of the cubes. In the case of closed cell foams, the cubic model considers the material to be shared among the channels and the cell walls, which translates to the edges and the faces of the cube. The closed cell also considers the effect of gas pressure in the cell providing additional stiffness. The ratio of solid material in the channels to material in the cell wall is denoted by $\phi$ in the Gibson-Ashby model equations. Equation 1 shows the relative elastic modulus of an open cell solid foam as a function of its relative density using the Gibson-Ashby model [5]. Equation 2 shows the relative elastic modulus of a closed cell solid foam as a function of its relative density using the Gibson-Ashby model [5]. Equation 3

shows the relative strength of an open cell solid foam as a function of its relative density using the Gibson-Ashby model [5]. Equation 4 shows the strength of a close cell solid foam as a function of its relative density using the Gibson-Ashby model [5]:

$$\frac{E_{Foam}}{E_{Solid}} \approx \left(\frac{\rho_{Foam}}{\rho_{Solid}}\right)^2 \quad (1)$$

$$\frac{E_{Foam}}{E_{Solid}} \approx \left(\phi\frac{\rho_{Foam}}{\rho_{Solid}}\right)^2 + (1-\phi)\frac{\rho_{Foam}}{\rho_{Solid}} + \frac{\rho_{Gas}(1-2\nu)}{E_{Solid}\left(1-\frac{\rho_{Foam}}{\rho_{Solid}}\right)} \quad (2)$$

$$\frac{\sigma_{Foam}}{\sigma_{Solid}} \approx 0.3\left(\frac{\rho_{Foam}}{\rho_{Solid}}\right)^{3/2} \quad (3)$$

$$\frac{\sigma_{Foam}}{\sigma_{Solid}} \approx 0.3\left(\phi\frac{\rho_{Foam}}{\rho_{Solid}}\right)^{\frac{3}{2}} + 0.4(1-\phi)\frac{\rho_{Foam}}{\rho_{Solid}} + \frac{p_{Gas}-p_{Atm}}{\sigma_{Solid}} \quad (4)$$

Here $E$ is the elastic modulus, ρ is the material density, $p$ is the pressure and ν is Poisson's ratio of the solid material, where the subscript 'Foam' denotes a bulk property of the solid foam, the subscript 'Solid' denotes a bulk property of the solid material in the foam and the subscript 'Gas' denotes a property of the gas in the cell. For typical values of $\phi$ closed cell structures provide superior mechanical strength and high elastic moduli.

More recent studies into solid foam structures have indicated that in some conditions the Gibson-Ashby model may be overestimating the mechanical properties of solid foams. Fischer et al [28] proposed an FE model based on a repeating Kelvin foam structure which provided a much closer match with experimental data. The parameters of the Kelvin foams were derived from X-ray micro-CT scanning of the PVC foams.

### *2.4 Thermal Properties*

Foams are used in many thermal applications as an insulating material. As such the thermal properties of foams have been extensively investigated. Heat transportation through a closed cell solid foam can be considered as the sum of all the heat transportation paths [5], [29]. The contributing heat transportation paths in a solid foam are: thermal conductivity through the solid material in the foam, thermal convection through the gas in the cell, thermal conductivity through the gas in the cell and radiative heat transfer between the faces of the cells. Heat transportation due to thermal conduction through the solid material is proportional to the relative density of the foam. Heat transportation due to convection in the gas in the cells is typically negligible as the small pockets of gas have small Grahof numbers. Moreover, the heat transported due to conduction through the gas is proportional to one minus the relative density of the solid foam. The heat transported due to radiation increases as the cell walls become more transparent. Hence the radiative heat transportation increases as the relative density of the foam decreases. As pointed out by a case study in chapter 7 'Cellular Solid: Structure and Properties' in reference [5], the increase in heat conducted via the solid material and the decrease in heat conducted via the gas and transferred through the structure as the relative density of the foam increases leads to an optimal foam relative density for thermal insulation.

The specific heat of a solid foam can be estimated by considering the specific heat and relative masses of the materials in the solid foam [5]. Even for very low relative density foams the mass contribution of the cell gas in the foams is very low, hence the specific heat of a solid foam is typically very similar to that of the solid material used in the foam.

### *2.5 Additional Properties*

Solid foams have been investigated for applications that are not thermal or mechanical, due to other advantageous properties. Some of these additional properties are intrinsic to solid foam materials, while others have been added to solid foam materials via a range of processes. An example of this is the carbon foam used by Moglie et al [30] for electromagnetic shielding.

### *2.6 Solid Foams in Vacuum*

The manufacturing of solid foams in space was explored by the REDEMPTION mission as reported by Candini et al [31] and later by Valdatta et al [32]. The REDEMPTION mission explored the use of PU foams, manufactured via the mixing of reactants. The mission planned to use solid foams as a method for capturing and attaching space debris to a de-orbiting satellite. To test the solid foams for this mission REDEMPTION carried out a series of experiments to examine the manufacturing of solid foams in space. This included a successful demonstration of manufacturing solid foams in vacuum. The PU resin was adapted for vacuum by reducing the blowing agent produced during the resin mixing. The vacuum manufactured solid foam process was intended to be tested on a sub-orbital rocket, however this test could not be carried out due to technical issues during the launch.

### *2.7 Solid Foams in micro-gravity*

There have been several studies investigating the development of both solid and liquid foams. As pointed out in section 2.2, the structures of many solid foams are formed during the liquid foam stage, hence studies exploring the effects of microgravity on liquid foams are relevant when discussing in-space manufacturing of solid foams. One such study of liquid foam carried out in microgravity was the FOCUS experiment, as discussed by Somosvári et al [33].

These experiments considered the development and life span of liquid foams produced on the ISS compared with foams produced on the ground. It was found that there were only minimal differences.

Solid foam production has also been considered in microgravity. A study by Quadrini et al [34] considered foams produced in hyper-gravity (in a centrifuge) to estimate the effects of microgravity on the formation of resin-based foams. It was concluded that micro-gravity is likely to have very little effect on the formation of such resin foams. While this study did not directly observe the effects of micro-gravity on solid foams it is in general agreement with studies that have observed the formation of liquid foams in micro-gravity.

## 3 In-Space Solid Foams Applications

As discussed, two of the key advantages of solid foams are their high packing ratio and rapid production time. As such solid foams could be used to quickly produce a large volume from limited feed stock.

The high specific strength and low thermal conductivity provided by solid foams has resulted in foam being suggested for use as an aeroshell designed for aerocapture [35]. The solid foam would allow for the construction of a very large rigid structure with a low mass and hence a low ballistic coefficient. Additionally, the low thermal conductivity of the foam could enable it to be used as a light weight thermal protection system.

As is discussed in section 4 solid foams could find applications as a thermal insulator given their low thermal conductivity [5]. Such applications could include sunshades or insulation for large human habitats in-orbit or on the surface of a planet. Given that foams have short production times they could be used to create an initial protective shell like that described by Boyd et al [36]. Inside this shell other, more sensitive, on-orbit manufacturing processes could take place.

As foams have a low density, they can be designed to have high specific flexural rigidity, as the same mass of material can provide a thicker section. This means that foams could be used to rigidise flexible components. In this manner solid foams could be used to deploy a large gossamer solar array similar to that described by Sproewitz et al [37].

Solid foams have been used for energy absorption during impacts or crashes [5], [38], [39]. A solid foam structure could replace the landing structure on an asteroid lander similar to that discussed by Zhao et al [40]. A suitable solid foam absorption layer could provide omnidirectional protection during landing, this could be very significant on objects with an uneven surface.

## 4 Case Studies

To investigate the use of in-space manufactured solid foams it is important to compare solid foam production to other processes that have been suggested for in-space manufacturing. This comparison has attempted to account for the full system requirements (such as energy consumption, construction time or mission mass).

### *4.1 Cantilever Beam*

A cantilever beam under a bending load can be used to make a comparison between different in-space manufacturing methods. Such a beam could, for example, have a torque applied to a large structure during an attitude slew manoeuvre. For this comparison we will consider the use of foam, FDM and DED printers used to manufacture beams in-space using foam (PU), plastic (PEEK) and metal (stainless steel) materials respectively. Each of the beams will use a square section as described in Figure 2 below.

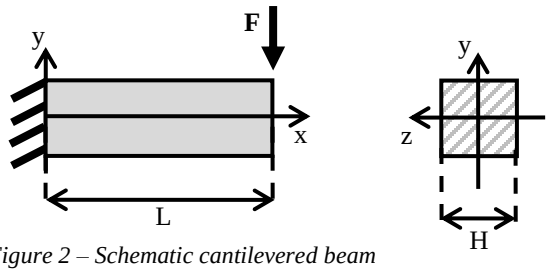


*Figure 2 – Schematic cantilevered beam*

Here *L* is the length of the beam, *H* is the thickness of the beam and *F* is the load applied to the beam. Each beam will be designed to support a bending load with a Factor of Safety (FoS) of 2 on the yield tensile strength as described in Equation 5:

$$FoS = \frac{\sigma_{Yield}}{\sigma_{Max}} \quad (5)$$

Here $\sigma_{Max}$ is the maximum tensile stress experienced by the beam and $\sigma_{Yield}$ is the tensile yield strength. Euler-Bernoulli beam theory can be used to calculate the thickness a square beam required to support a given load as described by Equation 6:

$$H = \sqrt[3]{\frac{6\,F\,L\,FoS}{\sigma_{Yeild}}} \quad (6)$$

The thickness of the beam can then be used to find the volume and mass of the beam, based on the density of the material used. Table 1 shows the thickness, volume and mass of a 1m long beam supporting a 1N load at the unsupported end.

*Table 1 – Cantilever beam performance*

| | Foam | FDM | DED |
|---|---|---|---|
| **Thickness (mm)** | 18.2 | 5.2 | 2.8 |
| **Beam Volume ($m^3$)** | $3.3\times10^{-4}$ | $2.7\times10^{-5}$ | $7.7\times10^{-6}$ |
| **Tensile Yield Strength (MPa)** | 1.99[a] | 87.34[b] | 558[c] |
| **Density ($kg/m^3$)** | 160[a] | 1300[d] | 7990[c] |
| **Beam Mass (g)** | 53.0 | 34.6 | 61.8 |

[a] Based on PCF10 as reported by Horak et al [6]
[b] Based on FDM printed PEEK 450G™ as report by Li and Lou [41]
[c] Based on DED printed stainless steel 316 (vertically printed) as reported by Zhang et al [42]
[d] Based on Vitex™ PEEK 450G™ [43]

As can be seen in Table 1, a greater mass of foam is required to support the cantilever beam. It is important to note that the material properties used in this example have been taken from terrestrial experiments, whereas the material may behave differently when manufactured and operated in-orbit.

The cantilever beam can be examined still further by considering the demands that each of these processes would place on the manufacturing system. The volume print rates of the FDM printer and the DED printer can be estimated based on the machine parameters discussed by Li and Lou [41] and Zhang et al [42] respectively. This estimated volume print rate is then used to find the total time required to print the beams. In the case of the DED and foam printing process the power required to run their respective printing process can be estimated, so the energy required for each process to manufacture the beam can be estimated as the product of the operational power and time. In the case of the FDM printing process the energy required to manufacture the beam was estimated by taking the product of the specific energy required to melt PEEK, starting from an ambient temperature of 23°C, and the mass of the beam. This estimation does not consider any loss in the FDM process or any additional power required to run non-heating equipment. The system requirement to print the beam on each of these printing processes are shown in Table 2.

As shown in Table 2 the foam beam can be produced for much less energy and in a much shorter time. When considering that a large structure may have hundreds of beams, the impact of a shorter lead time and low energy consumption for each beam could have a significant impact on the total time and energy required. These examples are based on one printer in each case, whereas it may be possible to print such structures quicker with more printers or a higher capacity printing process, but this would require a higher power consumption.

*Table 2 – System requirements for printing of cantilever beam*

| | Foam | FDM | DED |
|---|---|---|---|
| **Volume Print Rate ($mm^3/s$)** | $1\times10^{6}$ | 1.61 | 1.69 |
| **Mass Print Rate (g/s)** | 160 | $2.1\times10^{-3}$ | $1.4\times10^{-2}$ |
| **Print Time (s)** | 100[a] | $1.6\times10^{4}$ | $4.6\times10^{3}$ |
| **Power (W)** | 10 | N/A[b] | 1000 |
| **Energy (kJ)** | .01 | 23.3 | 456.8 |

[a] The foam has a minimum cure time of 80s and an additional 20s to lay down the material
[b] There is no direct power value for the FDM printer

### *4.2 Sunshade*

The use of foam in thermal applications can be explored by considering a sunshade as a case study. Such a sunshade could be used to block sunlight from sensitive payloads. A macro-scale sunshade, like that described here, would be capable of shading a large area and hence provide protection to large instruments such as space telescopes.

To understand the manufacturing parameters of large sunshades two manufacturing approaches have been considered: a thin-film sunshade and a foam sunshade. Both sunshades are squares with 150m edges. The thin-film design consists of two thin-film layers supported by a lightweight printed tensioning frame. The thin-film layers are made of aluminium using PVD while the frame is made of PEEK and is printed using FDM. It is assumed that there is little heat transportation through the tensioning frame and that the only heat transportation between the two layers is provided via radiation. The modelled uses the Stefan-Boltzmann law [44] to capture this heat exchange. The PVD process is similar to that described by Lippman [4]. The design of the tensioning frame is also similar to that investigated by Sleight and Muheim [45] for a solar sail. Figure 3 shows a schematic of the foam sunshade. Table 3 lists the foam sunshade's key parameters.

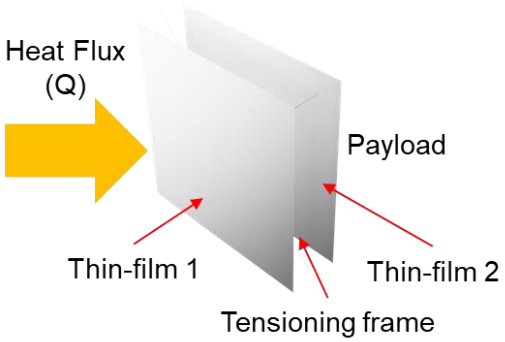


*Figure 3 – Thin-film sunshade*

*Table 3 – Thin-film sunshade parameters*

| Property | Value |
|---|---|
| **Thin-film thickness (μm)** | 2.5 |
| **Thin-film area (m2)** | $4.5\times10^{4}$ |
| **Thin-film density (kg/m3)** | 2700 |
| **Thin-film mass (kg)** | 304 |
| **Thin-film emissivity** | 0.04 |
| **Tensioner frame mass (kg)** | 171 |
| **Total mass (kg)** | 475 |

The foam shade is made of polyurethane and constructed in a similar manner to the beam discussed in section 4.1. The thermal properties of the polyurethane foam have been taken from Gibson and Ashby [5]. Figure 4 shows a schematic of the foam sunshade. Table 4 lists the foam sunshade's key parameters.

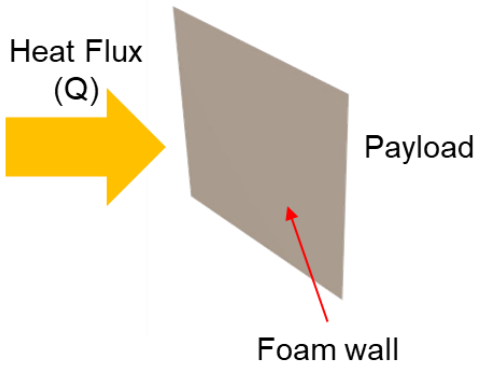


*Figure 4 – Foam sunshade*

*Table 4 – Foam sunshade parameters*

| Property | Value |
|---|---|
| **Foam thickness (mm)** | 173 |
| **Foam area ($m^2$)** | $2.3\times10^{4}$ |
| **Foam density ($kg/m^3$)** | 160 |
| **Foam thermal conductivity (W/m K)** | 0.025 |
| **Foam mass (kg)** | $6.2\times10^{4}$ |

Both sunshades have been designed to have a thermal resistance $R_T$ of $3\times10^{-5}$ K/W using Equation 7:

$$R_T = \frac{T_{Sun} - T_{Payload}}{Q} \quad (7)$$

Here $R_T$ is the thermal resistance, $T_{Sun}$ is the temperature of the shade on the surface facing the sun, $T_{Payload}$ is the temperature of the surface of the shade facing the payload and Q is the heat flux, in this case the solar flux. This would result in an R-Value (the area specific value of thermal resistance) of 0.69 $Km^2/W$. The manufacturing parameters of the two approaches are shown in Table 5 below. The manufacturing parameters of the PVD process have been taken from Lippman [4].

*Table 5 – Sunshade manufacturing parameters*

| Property | Thin film system | | | Foam |
|---|---|---|---|---|
| | Al PVD | PEEK FDM | Total | |
| **Mass print Rate (g/s)** | $5.6\times10^{-2}$ | $2.1\times10^{-3}$ | - | 213 |
| **Power (W)** | 2640 | 100 | - | 100 |
| **Print time (s)** | $5.4\times10^{6}$ | $8.2\times10^{7}$ | $8.7\times10^{7}$ | $2.9\times10^{5}$ |
| **Energy used (kJ)** | $1.4\times10^{7}$ | $8.2\times10^{6}$ | $2.3\times10^{7}$ | $2.9\times10^{4}$ |
| **Mass (kg)** | 304 | 171 | 475 | $6.2\times10^{4}$ |

As seen from Table 5, the foam sunshade takes less time and energy to produce when we consider the use of one printer. However, the foam sunshade requires considerably more mass than the thin-film approach. The foam would require less than 4 days of continuous manufacturing time, whereas the thin-film shade would require almost 3 years. This difference in print times and mass is so considerable that the two manufacturing approaches may be best used for different mission concepts. The foam process could be used for shorter duration missions in which a short

construction time is critical to returns on the mission, for example missions in LEO or MEO. The thin-film shade may be more suitable for longer duration missions in which the mass of the platform is critical, for example missions beyond Earth orbit.

A hybrid approach could also be envisaged where the foam is used in the structure of the tensioning frame, as opposed to the insulating layer itself. Such an approach could reduce the print time and energy required for the construction of the thin-film shade since most of the time taken (94%) and much of the energy consumed (36%) in constructing the thin-film shade is taken constructing the tensioning frame using FDM. A foam printing process could reduce the over all time and energy required to manufacture the Sunshade. As a blanket coverage of foam is not required the overall mass of the hybrid foam thin-film shade would be considerably less than the pure foam shade. However, this foam shade frame would most likely have a greater mass than the PEEK frame.

## 5 Conclusions

Solid foam manufacturing in space is potentially a key technology of interest for in-space manufacturing. The solid foam printing process holds the promise of providing large-scale, lightweight structures with low mass, that could be printed in short timescales with significantly less energy than other methods proposed for in-space manufacturing. The solid foam material produced also provides interesting thermal and mechanical properties that could be used in a range of thermal-mechanical applications.

Further study is required to fully understand the likely properties of solid foams produced in space. The results of such research would be critical in the design and construction of a full-scale planer foam structure in space. Simulations of both the micro-scale solid foam structure and the macro-scale planar structure would be critical to understanding the material properties of a solid foam produced in space and the behaviour of a solid foam structure that is too large to test in a laboratory.

**Acknowledgments**

The work report in this paper was supporting by funding from the Royal Academy of Engineering under the Chair in Emerging Technologies scheme.

**References**

[1] R. Skomorohov, A. M. Hein, and C. Welch, ‘In-orbit Spacecraft Manufacturing: Near-Term Business Cases’, Sep. 2016.

[2] M. McRobb, B. Robb, S. Ridley, and C. McInnes, ‘Emerging Space Technologies: Macro-scale On-orbit Manufacturing’, in *Enabling Technologies*, Belfast, Northern Ireland, Nov. 2019, vol. BIS-RS-2019-07, pp. 1–5. Accessed: Apr. 13, 2021. [Online]. Available: http://eprints.gla.ac.uk/204190/

[3] T. Prater, N. Werkheiser, F. Ledbetter, D. Timucin, K. Wheeler, and M. Snyder, ‘3D Printing in Zero G Technology Demonstration Mission: complete experimental results and summary of related material modeling efforts’, *Int J Adv Manuf Technol*, vol. 101, no. 1, pp. 391–417, Mar. 2019, doi: 10.1007/s00170-018-2827-7.

[4] M. E. Lippman, ‘In-space fabrication of thin-film structures’, 1972.

[5] L. J. Gibson and M. F. Ashby, *Cellular solids: structure and properties*, 2nd ed. Cambridge: Cambridge University Press, 1997.

[6] Z. Horak, K. Dvorak, L. Zarybnicka, H. Vojackova, J. Dvorakova, and M. Vilimek, ‘Experimental Measurements of Mechanical Properties of PUR Foam Used for Testing Medical Devices and Instruments Depending on Temperature, Density and Strain Rate’, *Materials*, vol. 13, no. 20, Art. no. 20, Jan. 2020, doi: 10.3390/ma13204560.

[7] R. Kumar *et al.*, ‘Improved microwave absorption in lightweight resin-based carbon foam by decorating with magnetic and dielectric nanoparticles’, *RSC Adv.*, vol. 4, no. 45, pp. 23476–23484, Jun. 2014, doi: 10.1039/C4RA01731E.

[8] J. Luyten, S. Mullens, J. Cooymans, A. M. De Wilde, I. Thijs, and R. Kemps, ‘Different methods to synthesize ceramic foams’, *Journal of the European Ceramic Society*, vol. 29, no. 5, pp. 829–832, Mar. 2009, doi: 10.1016/j.jeurceramsoc.2008.07.039.

[9] M. F. Ashby, A. G. Evans, N. A. Fleck, L. J. Gibson, J. W. Hutchinson, and H. N. G. Wadley, *Metal Foams: A Design Guide*. London: Butterworth-Heinemann, 2000.

[10] M. Antunes and J. I. Velasco, ‘Polymeric Foams’, *Polymers*, vol. 11, no. 7, Art. no. 7, Jul. 2019, doi: 10.3390/polym11071179.

[11] L. Cafiero, O. Alfano, M. Iannone, F. Esposito, S. Iannace, and L. Sorrentino, ‘Microcellular foams from PEEK/PEI miscible blends’, Graz, Austria, 2016, p. 090009. doi: 10.1063/1.4965568.

[12] Z. Ma, G. Zhang, Q. Yang, X. Shi, and A. Shi, ‘Fabrication of microcellular polycarbonate foams with unimodal or bimodal cell-size distributions using supercritical carbon dioxide as a blowing agent’, *Journal of Cellular Plastics*, vol. 50, no. 1, pp. 55–79, Jan. 2014, doi: 10.1177/0021955X13503849.

[13] A. H. Landrock, *Handbook of Plastic Foams: Types, Properties, Manufacture and Applications*. Elsevier, 1995.

[14] P. Rattanakawin *et al.*, 'Highly Ordered Nanocellular Polymeric Foams Generated by UV-Induced Chemical Foaming', *ACS Macro Lett.*, vol. 9, no. 10, pp. 1433–1438, Oct. 2020, doi: 10.1021/acsmacrolett.0c00475.

[15] S. Schlögl, M. Reischl, V. Ribitsch, and W. Kern, 'UV induced microcellular foaming—A new approach towards the production of 3D structures in offset printing techniques', *Progress in Organic Coatings*, vol. 73, no. 1, pp. 54–61, Jan. 2012, doi: 10.1016/j.porgcoat.2011.08.020.

[16] D. M. Wirth, A. Jaquez, S. Gandarilla, J. D. Hochberg, D. C. Church, and J. K. Pokorski, 'Highly Expandable Foam for Lithographic 3D Printing', *ACS Appl. Mater. Interfaces*, vol. 12, no. 16, pp. 19033–19043, Apr. 2020, doi: 10.1021/acsami.0c02683.

[17] J. Reignier, P. Alcouffe, F. Méchin, and F. Fenouillot, 'The morphology of rigid polyurethane foam matrix and its evolution with time during foaming – New insight by cryogenic scanning electron microscopy', *Journal of Colloid and Interface Science*, vol. 552, pp. 153–165, Sep. 2019, doi: 10.1016/j.jcis.2019.05.032.

[18] W. Drenckhan and S. Hutzler, 'Structure and energy of liquid foams', *Advances in Colloid and Interface Science*, vol. 224, pp. 1–16, Oct. 2015, doi: 10.1016/j.cis.2015.05.004.

[19] J. A. F. Plateau, *Statique expérimentale et théorique des liquides soumis aux seules forces moléculaires*. Gauthier-Villars, 1873.

[20] P. Stevenson, *Foam Engineering: Fundamentals and Applications*. Somerset, UNITED KINGDOM: John Wiley & Sons, Incorporated, 2012. Accessed: Nov. 16, 2020. [Online]. Available: http://ebookcentral.proquest.com/lib/gla/detail.action?docID=834623

[21] K. Yasunaga, R. A. Neff, X. D. Zhang, and C. W. Macosko, 'Study of Cell Opening in Flexible Polyurethane Foam', *Journal of Cellular Plastics*, vol. 32, no. 5, pp. 427–448, Sep. 1996, doi: 10.1177/0021955X9603200502.

[22] A. van der Net, A. Gryson, M. Ranft, F. Elias, C. Stubenrauch, and W. Drenckhan, 'Highly structured porous solids from liquid foam templates', *Colloids and Surfaces A: Physicochemical and Engineering Aspects*, vol. 346, no. 1, pp. 5–10, Aug. 2009, doi: 10.1016/j.colsurfa.2009.05.010.

[23] T. Azdast and R. Hasanzadeh, 'Increasing cell density/decreasing cell size to produce microcellular and nanocellular thermoplastic foams: A review', *Journal of Cellular Plastics*, p. 0021955X20959301, Sep. 2020, doi: 10.1177/0021955X20959301.

[24] M. Ridha, 'Mechanical and Failure Properties of Rigid Polyurethane Foam Under Tension', p. 227.

[25] M. Ridha and V. P. W. Shim, 'Microstructure and Tensile Mechanical Properties of Anisotropic Rigid Polyurethane Foam', *Exp Mech*, vol. 48, no. 6, p. 763, Apr. 2008, doi: 10.1007/s11340-008-9146-0.

[26] M. S. Gholami, O. Doutres, and N. Atalla, 'Effect of microstructure closed-pore content on the mechanical properties of flexible polyurethane foam', *International Journal of Solids and Structures*, vol. 112, pp. 97–105, May 2017, doi: 10.1016/j.ijsolstr.2017.02.016.

[27] J. Storm *et al.*, 'Geometrical modelling of foam structures using implicit functions', *International Journal of Solids and Structures*, vol. 50, no. 3, pp. 548–555, Feb. 2013, doi: 10.1016/j.ijsolstr.2012.10.026.

[28] F. Fischer, G. T. Lim, U. A. Handge, and V. Altstädt, 'Numerical Simulation of Mechanical Properties of Cellular Materials Using Computed Tomography Analysis', *Journal of Cellular Plastics*, vol. 45, no. 5, pp. 441–460, Sep. 2009, doi: 10.1177/0021955X09339340.

[29] M. A. Schuetz and L. R. Glicksman, 'A Basic Study of Heat Transfer Through Foam Insulation', *Journal of Cellular Plastics*, vol. 20, no. 2, pp. 114–121, Mar. 1984, doi: 10.1177/0021955X8402000203.

[30] F. Moglie, D. Micheli, S. Laurenzi, M. Marchetti, and V. Mariani Primiani, 'Electromagnetic shielding performance of carbon foams', *Carbon*, vol. 50, no. 5, pp. 1972–1980, Apr. 2012, doi: 10.1016/j.carbon.2011.12.053.

[31] G. P. Candini *et al.*, 'REDEMPTION: a microgravity experiment to test foam for space debris removal', Cape Town, SA, Oct. 2011, vol. 3.

[32] M. Valdatta *et al.*, 'Inflatable System Based on Polyurethanic Foam', Naples, Italy, Jan. 2013, vol. 721, pp. 153–160.

[33] B. M. Somosvári, P. Bárczy, J. Szóke, P. Szirovicza, and T. Bárczy, 'FOCUS: Foam evolution and stability in microgravity', *Colloids and Surfaces A: Physicochemical and Engineering Aspects*, vol. 382, no. 1, pp. 58–63, Jun. 2011, doi: 10.1016/j.colsurfa.2011.01.035.

[34] F. Quadrini, G. M. Tedde, L. Santo, and J. J. W. A. van Loon, 'Solid-state foaming of epoxy resin under hypergravity and simulated microgravity', *Advances in Polymer Technology*, vol. 37, no. 7, pp. 2616–2624, 2018, doi: https://doi.org/10.1002/adv.21937.

[35] P. Hastie, G. Bailet, C. White, and C. R. McInnes, 'The Use of In-Space Manufactured Solid Foams for Aerocapture', presented at the 18th International Planetary Probe Workshop, 2021. Accessed: Aug. 26, 2021. [Online]. Available: https://drive.google.com/file/d/16jTDSiqqslnTxWTPcBx4QBqwFq_JKTIL/edit

[36] I. D. Boyd, R. S. Buenconsejo, D. Piskorz, B. Lal, K. W. Crane, and E. De La Rosa Blanco, 'On-Orbit Manufacturing and Assembly of Spacecraft', The Institute for Defence Analyses, Washington DC, IDA Paper P-8335, Jan. 2017. [Online]. Available: https://www.ida.org/-/media/feature/publications/o/on/on-orbit-manufacturing-and-assembly-of-spacecraft/on-orbit-manufacturing-and-assembly-of-spacecraft.ashx

[37] T. Sproewitz *et al.*, 'Concept for a Gossamer solar power array using thin-film photovoltaics', *CEAS Space J*, vol. 12, no. 1, pp. 125–135, Jan. 2020, doi: 10.1007/s12567-019-00276-6.

[38] P. Sakthivel, S. R. Diliphan, P. Ruthrasagar, M. S. Prakash, and A. Vignesh, 'Experimental Analysis of Circular Hollow Steel Pipe Filled with Polyurethane Foam in Automotive Applications', no. 5, p. 6, 2021.

[39] S. Li and Q. M. Li, 'Response of functionally graded polymeric foam under axial compression', *International Journal of Mechanical Sciences*, p. 106750, Aug. 2021, doi: 10.1016/j.ijmecsci.2021.106750.

[40] Z. Zhao, J. Zhao, and H. Liu, 'An asteroid landing mechanism and its landing simulation', in *2012 IEEE International Conference on Robotics and Biomimetics (ROBIO)*, Dec. 2012, pp. 205–210. doi: 10.1109/ROBIO.2012.6490967.

[41] Y. Li and Y. Lou, 'Tensile and Bending Strength Improvements in PEEK Parts Using Fused Deposition Modelling 3D Printing Considering Multi-Factor Coupling', *Polymers*, vol. 12, no. 11, Art. no. 11, Nov. 2020, doi: 10.3390/polym12112497.

[42] K. Zhang, S. Wang, W. Liu, and X. Shang, 'Characterization of stainless steel parts by Laser Metal Deposition Shaping', *Materials & Design*, vol. 55, pp. 104–119, Mar. 2014, doi: 10.1016/j.matdes.2013.09.006.

[43] Victrex plc, 'Victrex™ PEEK 450G™'. Nov. 2019. [Online]. Available: http://www.victrex.com/

[44] D. G. Gilmore, Ed., *Spacecraft Thermal Control Handbook*, Second., vol. 1. El Segundo, California: The Aerospace Press, 2002. Accessed: Apr. 15, 2021. [Online]. Available: https://www.academia.edu/934756/Thermal_Control_Handbook

[45] D. Sleight and D. Muheim, 'Parametric Studies of Square Solar Sails Using Finite Element Analysis', presented at the 45th AIAA/ASME/ASCE/AHS/ASC Structures, Structural Dynamics & Materials Conference, Palm Springs, California, Apr. 2004. doi: 10.2514/6.2004-1509.